AIP ADVANCES 7, 015117 (2017)

Carrier delocalization in InAs/InGaAlAs/InP quantum-dash-based tunnel injection system for 1.55 μm emission

W. Rudno-Rudziński,[1,a] M. Syperek,[1] J. Andrzejewski,[1] A. Maryński,[1] J. Misiewicz,[1] A. Somers,[2] S. Höfling,[2,3] J. P. Reithmaier,[4] and G. Sęk[1]

[1]*Department of Experimental Physics, Faculty of Fundamental Problems of Technology, University of Science and Technology, St. Wyspiańskiego 27, 50-370 Wrocław, Poland*

[2]*Technische Physik, University of Würzburg and Wilhelm-Conrad-Röntgen-Research Center for Complex Material Systems, Am Hubland, D 97074 Würzburg, Germany*

[3]*SUPA, School of Physics and Astronomy, University of St. Andrews, North Haugh, KY16 9SS St. Andrews, United Kingdom*

[4]*Institute of Nanostructure Technologies and Analytics, Technische Physik, Universitaet Kassel, Heinrich-Plett-Str. 40, 34132 Kassel, Germany*

(Received 20 October 2016; accepted 23 January 2017; published online 31 January 2017)

We have investigated optical properties of hybrid two-dimensional-zero-dimensional (2D-0D) tunnel structures containing strongly elongated InAs/InP(001) quantum dots (called quantum dashes), emitting at 1.55 μm. These quantum dashes (QDashes) are separated by a 2.3 nm-width barrier from an InGaAs quantum well (QW), lattice matched to InP. We have tailored quantum-mechanical coupling between the states confined in QDashes and a QW by changing the QW thickness. By combining modulation spectroscopy and photoluminescence excitation, we have determined the energies of all relevant optical transitions in the system and proven the carrier transfer from the QW to the QDashes, which is the fundamental requirement for the tunnel injection scheme. A transformation between 0D and mixed-type 2D-0D character of an electron and a hole confinement in the ground state of the hybrid system have been probed by time-resolved photoluminescence that revealed considerable changes in PL decay time with the QW width changes. The experimental discoveries have been explained by band structure calculations in the framework of the eight-band **k**·**p** model showing that they are driven by delocalization of the lowest energy hole state. The hole delocalization process from the 0D QDash confinement is unfavorable for optical devices based on such tunnel injection structures. [http://dx.doi.org/10.1063/1.4975634]

Hybrid systems comprising quantum dots (QDs) being an active element and a quantum well (QW), serving as a reservoir of carriers to be injected to QDs through a thin barrier, are called tunnel injection (TI) structures. The combination of quasi-0D confinement potential in QDs and the 2D one in a QW constitutes an interesting object for investigation of fundamental physics of coupled nanostructures with different dimensionality, and practical applications in optoelectronic devices, e.g. lasers. Carefully designed TI structures make possible taking advantage of improved characteristics of a QD-based laser, such as lower threshold current,[1,2] better temperature stability[3–5] and wider spectral tunability,[6] while addressing the issue in QD lasers that hinders their performance, i.e. limited modulation rates due to considerable population of hot carriers occupying QD excited states and wetting layer states. The tuning of the TI energy structure in such a way that the lowest energy electron state in the QW is an optical phonon energy above the QD ground state (GS), supported by *p*-doping, offers a fast and efficient supply of cold electrons, enabling broad bandwidth devices.[7,8]

[a]corresponding author e-mail: wojciech.rudno-rudzinski@pwr.edu.pl

Tunnel injection based lasers have also been demonstrated to exhibit high power,[9] ultralow threshold[10] and broad tunability in a comb scheme.[11]

Many material systems involving QW-QD coupling have been investigated, e.g. GaN-based UV[12] and visible[13] sources; visible InP/InGaP-based external grating lasers;[14] InAs/GaAs QDs emitting at 1.3 μm coupled to a dilute nitride injector QW;[15,16] highly demanded InAs/InP QDs for the emission at 1.55 μm.[17,18] However, works are usually focused only on emission properties, especially laser gain characteristics, without detailed investigations of the underlying physics. The bulk of articles on TI structures concerns a model InAs/GaAs QD system,[19–23] with an InGaAs QW injector, which however is less appealing for practical applications due to a limitation in the emission wavelength. There exist also a few papers presenting numerical simulations of TI structures, mostly focused on gain characteristics and dynamic response of TI based lasers,[24] including structures with double injection QWs.[25] Ref. 26 shows a detailed analysis of phonon-assisted tunneling to InGaAs QDs. A QW-QD hybrid system may be also used for achieving ultrafast injection of polarized spins[27] or as active regions for semiconductor optical amplifiers, in order to decrease the time of gain recovery, crucial for high speed devices.[28] The study of coupling between QDs and QW is also interesting from the point of view of QD-based memories,[29] infrared photodetectors[30] and quantum-dot-based quantum cascade lasers.[31]

We present here comprehensive experimental and theoretical studies on InP-based TI structures containing InAs quantum dashes (QDashes). These structures substantially differ from typical quantum dots since they are strongly elongated in [1-10] direction and hence they have a denser ladder of confined states.[32,33] In the considered design, QDashes are immersed in the InGaAlAs matrix, with the GS emission near 1.55 μm at room temperature (RT). We investigate three structures that contain a single $In_{0.53}Ga_{0.47}As$ injector QW with different thicknesses, translating into decreasing energy difference between the lowest injector state and the QDash GS. The goal of the article is to investigate the influence of an injector on the band-structure of the coupled system, in particular, its GS. We point out at an issue of the spatial extent of the probability densities of the GS wavefunctions for both types of carriers, which are deduced from the measurement of an e-h lifetime and confirmed by numerical calculations in the 3D eight-band $\mathbf{k}\cdot\mathbf{p}$ model. This knowledge, not available in the literature for InAs/InGaAlAs/InP material system, is crucial to understand physical properties of TI structures, which govern operating parameters of future devices.

Tunnel injection structures were grown in an EIKO gas source molecular beam epitaxy (MBE) system on (001) sulfur-doped InP substrates. Directly on the substrate a 200 nm thick $In_{0.53}Al_{0.47}As$ buffer layer, followed by a 30 nm thick $In_{0.53}Ga_{0.23}Al_{0.24}As$ layer, were grown. Then, an $In_{0.53}Ga_{0.47}As$ layer was deposited. Its thickness is changed between the samples, forming a 4.5, 5.5 and 6.5 nm thick QW, respectively. The QW is followed by a 1.7 nm thin $In_{0.53}Al_{0.47}As$ layer and a 0.6 nm $In_{0.53}Ga_{0.23}Al_{0.24}As$ layer, constituting together a tunneling barrier. Subsequently, QDashes where formed in the Stranski-Krastanow growth mode by deposition of a nominally 1.05 nm-thick InAs layer, that resulted in a formation of a thin (~1 nm) wetting layer and ~3.5 nm-high QDashes. The self-assembled QDashes were then covered with a 30 nm thick $In_{0.53}Ga_{0.23}Al_{0.24}As$ layer, 100 nm $In_{0.53}Al_{0.47}As$ layer and a 10 nm InP cap layer. All the layers, except for the QDash one (InAs material), are lattice matched to InP. Growth details, as well as optical and electronic properties of such QDashes, are described in the previously published articles.[34–36]

For photoluminescence (PL), photoluminescence excitation (PLE), and time-resolved photoluminescence experiments (TRPL), the samples were held in a continuous-flow liquid-helium cryostat at T = 5 K. In the PL experiment, the TI structures were excited above the InAlGaAs barrier by the 532 nm line from a neodymium-doped yttrium aluminum garnet laser. The resultant PL signal was dispersed by a 0.5-m-focal-length monochromator and measured with an InGaAs linear array detector. The PLE and TRPL experiments were performed in a similar way as in Ref. 37. For the PR experiment, a halogen lamp as a broadband source and a 630 nm line from a semiconductor diode laser for modulation were used. The light reflected off a sample was dispersed by a 0.5-m-focal-length monochromator and detected by an InGaAs p-i-n photodiode. The photoreflectance (PR) measures the change in the reflectivity spectrum upon photo-modulation, resulting in a derivative-like

response, with clear signatures of optical transitions.[36] The PR was performed at both T = 5 K and RT, however, at low temperature the PR signal (not shown) cannot be separated from the PL signal dominating the overall spectral response. At T=300 K, the PL process constitutes only a background of the pronounced PR amplitude. To compare optical response of the TI structures between various experiments conducted at low T, there are used the RT PR spectra, corrected in energy to compensate for the thermal changes in QW and QDash material band-gaps, responsible for most of the shift of levels confined considerably below the barrier energy.

Before the discussion on spectroscopic data, it is worth noticing that implementation of the TI scheme requires careful tuning of the injector QW thickness to fulfill two conditions: (i) fast carrier relaxation/efficient carrier transfer down to the GS, and (ii) preservation of its quasi-0D character. The first condition requires electronic coupling between 2D QW and 0D QDash states. The coupling secures the carrier transfer process from the initially highly populated injector to QDashes, either directly to the QDash GS [preferably with an assistance of a longitudinal optical (LO) phonon, to decrease the probability of back-tunneling] or through excited state(s). The hole transfer in the valence band is not critical, since the ladder of confined hole states in InAs/InP QDashes is very dense, with states' separation in a single meV range,[38] facilitating fast hole relaxation down to the GS. The second condition assumes a strong confinement of the lowest energy states for both types of carriers in QDashes, ensuring the 0D character of emission. To evaluate those assumptions we

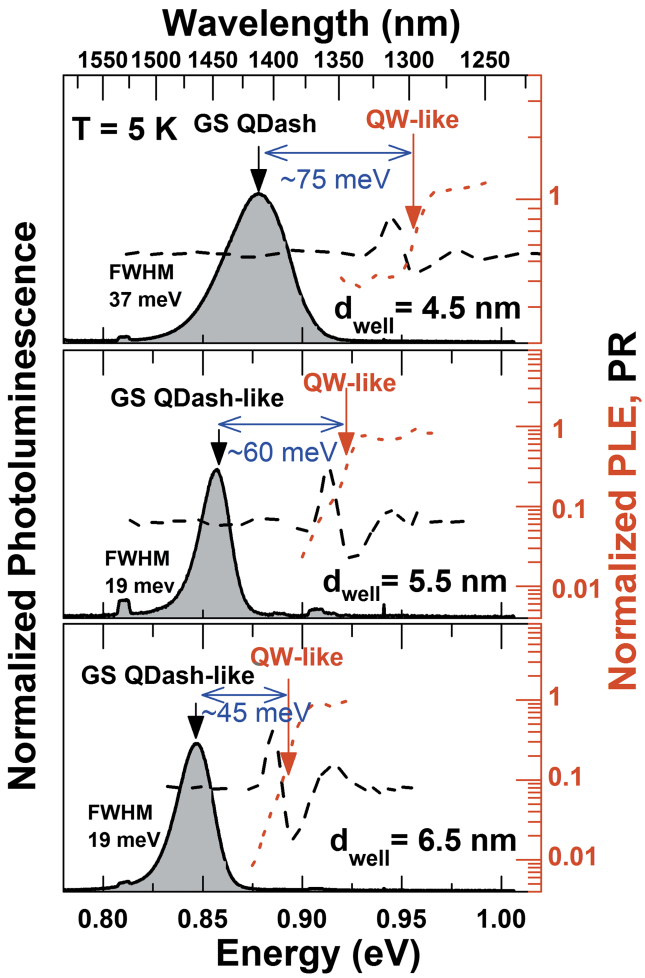

FIG. 1. Optical response for three TI structures, differing in QW thickness d_{well}. PL emission bands (solid shaded black lines) and PLE traces (dotted red lines) are measured at T = 5 K and P_{exc} = 300 μW. The PR (dashed black lines) is obtained at T = 300 K and spectraly shifted.

study three TI structures, differing in QW thickness (d_{well}) and thus affecting the coupling between QW and QDash confined states. Figure 1 shows the results of basic optical characterization in the energy range below the band gap of the $In_{0.53}Ga_{0.23}Al_{0.24}As$ barrier (<1.15 eV). Low-temperature PL spectra present emission bands for the GS of an entire TI structure that are centered at the energies (wavelengths) of 0.878 (1.412), 0.856 (1.448) and 0.846 eV (1.465 μm) for the samples with d_{well} = 4.5, 5.5 and 6.5 nm, respectively. If we only assume that unintentional variations in the growth conditions are negligible the apparent shift in the GS emission energy between TI structures may be explained by at least two factors: (i) the increased coupling between the QW and QDashes that should effectively broaden the confinement potential of QDashes, pushing down energy levels in accordance to the quantum size effect, and (ii) a change in the character of the GS transition from 0D-like for uncoupled TI structures to 2D-like for structures with a wide QW. The first factor cannot fully explain the experimental observation since the numerical calculations (described in details later) show that it accounts to just several meV. The second factor can be supported by experimentally observed change in the energy and broadening of the GS emission peak - 37 meV full width at half maximum for the sample with a d_{well} = 4.5 nm, contrary to just 19 meV for the other two, much less than the typical broadening for QDashes (~40 meV). Since such a considerable improvement in growth homogeneity between the TI samples by just changing the QW thickness is highly unlikely, the changes in the broadening must be attributed to other factors. The GS transition in the sample with a 4.5 nm thick QW seems to occur within 0D-like density of states (DOS), whereas the other two samples exhibit a mixed character of the GS transition, between 0D and 2D DOS, which will be explored later.

Next, PR experiment is employed to determine the lowest optical transition related to the QW-like reservoir of carriers for the TI GS. Respective experimental traces are depicted in Fig. 1. One can see only a very weak PR feature at the PL peak energy, which is common for the QDash-related signal due to a small total absorption of a single QDash layer and their large intrinsic nonuniformity.[36] In contrast, pronounced PR resonances can be identified for all the samples at higher energies, related to optical transitions within the mixture of 0D-2D DOS. The energy of these transitions increases with d_{well}, resulting in the decreasing spectral detuning between QW and QDash parts. The spectral detuning is measured as an energy difference between the lowest energy PR feature related to the QW and the center of the PL peak, and reaches approx. 75, 60, and 45 meV for d_{well}=4.5, 5.5, 6.5 nm, respectively. Figure 1 also shows the PLE amplitude detected at the maximum of GS emission for each TI structure. A sharp drop in its intensity coincides with the energy of the QW-related PR feature, indicating an efficient carrier transfer from the injector QW to the QDash layer above this energy.[18] Other shoulders in the PLE curve can be related to higher energy transitions in the QW system, also seen in the PR spectra. Below the QW-related transition energy, the GS may be populated through the absorption in QDash excited states.

The spectroscopic data confirm the existence of electronic coupling and thus carrier transfer between the QW and QDashes in the investigated TI structures, which fulfills the first condition required for a TI architecture. However, there remains to be verified if GS emission of the entire system still occurs between holes and electrons localized in the QDashes. Therefore, a TRPL experiment is performed at low pulse energy (~1 photon/dot) and quasi-resonant excitation at ~0.92 eV for TI structures with d_{well}=4.4, 5.5 nm, and ~0.88 eV for the one with d_{well}=6.5 nm. Consequently, e-h pairs are photo-created within the 0D-like DOS formed by excited states in the QDashes or a mixture of 0D and 2D DOS, as dictated by the electronic coupling. Figure 2(a) displays PL decay curves for all the samples, consisting of a fast PL rise and much longer decay, occurring in a few nanosecond time scale. The rise times are below the experimental resolution (~20 ps), indicating fast carrier relaxation into the GS. In the case of the TI structure with d_{well} = 4.5 nm, the PL decay can be well fitted with a mono-exponential decay function. The respective decay time constant is τ_{PL} = 2.0 ± 0.1 ns, as depicted in Fig. 2(b). This value agrees with measurements on single QDashes grown in analogous conditions (~2 ns)[39] and corresponds to the decay times calculated based on the strong confinement limit (~2.2 ns).[37,38] Consequently, the result points out at the emission from isolated 0D states, without any noticeable influence of the QDash environment. The situation changes for the samples with increasing QW thickness, where the PL decay does not have a clear mono-exponential character, already suggesting that the recombination is altered by the e-h confinement conditions. Although it

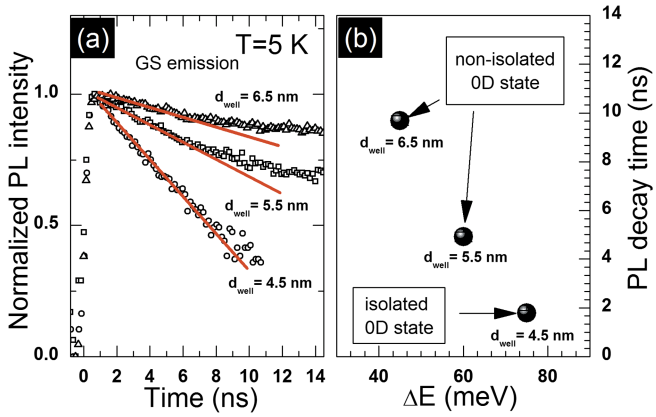

FIG. 2. (a) PL decay traces obtained at T = 5 K for three TI structures with QW width of 4.5, 5.5 and 6.5 nm. Red solid lines depict mono-exponential decay. (b) Extracted PL decay times (black dots) for the mono-exponential decay.

is hard to propose exact expression to determine the relevant parameters of such PL kinetics, we assume that at least in the range of 0-8 ns the PL decay can be treated as mono-exponential. It allows obtaining the respective decay time constants to 5.0±0.2 and 10.0±0.2 ns for the TI structures with d_{well}= 5.5 nm and 6.5 nm (see Fig. 2(b)). Similar results were also found for non-resonant excitation at ∼1.49 eV, above the InGaAlAs barrier, which suggests that under given experimental conditions the PL decay is mostly defined by the radiative lifetime. The substantial elongation of the decay time shown in Fig. 2(b) as a function of the spectral detuning between the PL peak emission and the PR feature suggests delocalization of the carriers' wavefunction out of the QDash confining potential with increasing the QW width.

To strengthen the interpretation of experimental results we calculated the first three lowest energy wavefunctions for both types of carriers. Although we neglect the Coulomb interaction between electron-hole pairs, the observed experimental results can still be explained in a qualitative way. The obtained transitions energies for all the samples are in satisfactory agreement with the experimental data (less than 15 meV difference). The calculations reveal that presence of the QW potential has an apparent influence on the GS energy of the entire hybrid system, causing a redshift of about 7 meV with increasing QW thickness. Figure 3 presents squares of moduli of the electron ($|\Psi_e|^2$) and hole state ($|\Psi_h|^2$) wavefunctions, integrated in the X-Y plane and superimposed on the cross-section of the effective potential through the middle of a QDash. The lowest energy electron states for all the samples are similar, showing substantial localization of the $|\Psi_e|^2$ in a QDash. However, for higher order states and with increasing well widths the contribution of the $|\Psi_e|^2$ into the QW part of the system increases. Such a distributed wavefunctions may constitute the channel for carrier transfer from the injector to QDashes. A qualitative difference between the investigated samples can be seen for hole states. The lowest-lying hole state of an entire TI structure is concentrated in the QDash when d_{well} = 4.5 nm, but for the samples with thicker QWs, the 'center-of-mass' for $|\Psi_h|^2$ shifts towards the QW part of the structure. This theoretical picture is directly confirmed by the results of the TRPL experiment. Spatial isolation of an e-h pair in the QDash is translated into relatively short PL lifetime, comparable to the exciton lifetime in typical QDash structures. Delocalization of the hole out of the QDash potential transforms the GS transition from direct to indirect in the real space, which is seen as an elongation of PL lifetimes for TI structures with d_{well} = 5.5 and 6.5 nm. The change of the character of the GS also explains the considerable narrowing of the GS emission from 37 meV down to 19 meV. The first value, corresponding to a direct optical transition, reflects the statistical distribution of individual QDash GS energies related to inhomogeneities in the QDash ensemble. In the second case, the final state of the transition is localized in the more homogeneous QW, resulting in the narrower PL emission peak.

These results show that the engineering of the electronic band structure of the hybrid system is very demanding. The system under study can have an unfavorable alignment of confined levels. If the GS transition becomes indirect in the real space it would imply low efficiency

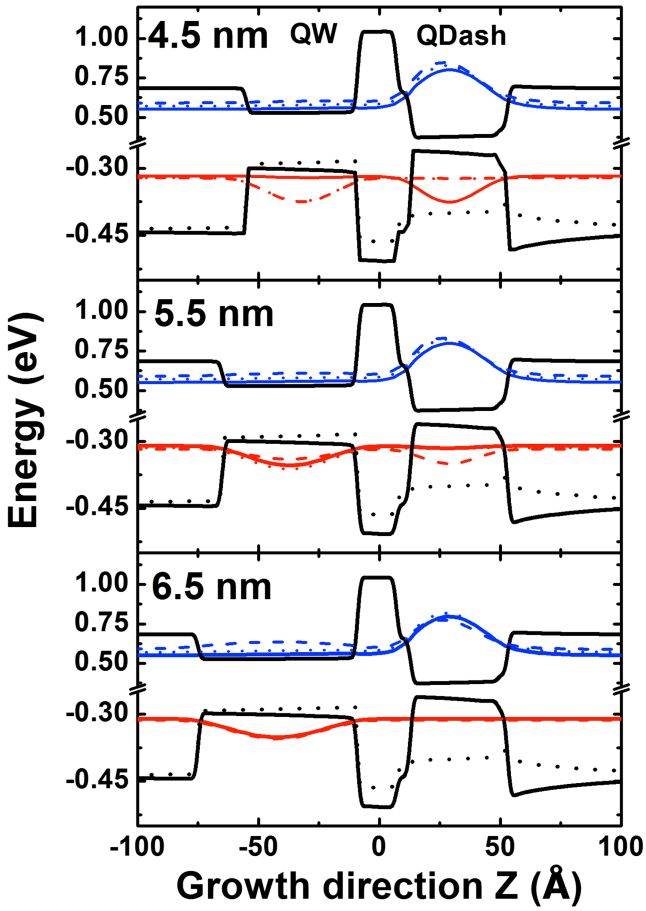

FIG. 3. Squared moduli of the lowest energy electron (blue) and hole (red) wave functions (integrated in X and Y directions), superimposed on the cross-section through the middle of the dash of strained valence and conduction band potentials. Solid line indicates the ground state, dotted lines the first excited state and dashed lines the second excited state. Dotted black lines indicate the potential for light holes.

of emission and reduced modulation speed, limiting practical application of investigated samples in lasers or optical amplifiers. Similar effects have been shown for other TI systems, based on InAs/GaAs[19] and InAs/InGaAsP[40] materials. Both reveal the elongation of the GS emission decay times with increased coupling, related to the GS transition becoming indirect in a real space. However, for all these systems it is caused by the leaking of $|\Psi_e|^2$ from the 0D-like nanostructure, showing that material parameters, mostly band offsets, play a crucial role and that proper engineering of TI structures requires careful design and further research. There are still many degrees of freedom to be utilized to improve this concept, i.a. one can change the barrier width and its height, or tune the properties of a quasi-0D potential by applying a more symmetric QD nanostructures.

In conclusion, we have studied the influence of QW width on electronic coupling in the InP-based tunnel-injection system composed of InAs quantum dashes separated by a thin barrier from an InGaAs QW, designed as a potential active part of lasers operating at 1.55 μm. We have shown that the coupling alters spectral and temporal optical response of the TI system by affecting the isolated 0D character of the GS emission for wide QWs. The well width remains an essential degree of freedom for tailoring the energy separation between the carrier reservoir and the GS of the entire TI system. However, for wide wells the GS transition becomes indirect, as viewed by the elongation of the PL decay time from ~2 ns up to ~10 ns. Numerical calculations have pointed at a delocalization of a hole state, spread between the QW and QDash confining potentials, while the electrons remain localized in the QDash. This unfavorable transformation is an obstacle on the way to achieving optimal architecture

of the TI system, where its particular advantages come from the 0D-like character of the GS emission. Yet, several structure parameters need further optimizations to improve the TI system design, e.g. well and barrier widths and their chemical compositions. Another approach can be to tailor the QD geometry and use more symmetric InAs/InP quantum dots that have successfully been grown by MBE in recent years.[41] The change in morphology, resulting e.g. in different strain distribution, will affect the electron and hole states differently influencing their localization and the coupling with the QW injector. Utilizing smaller QDs would have some additional advantages from the laser device performance point of view, as it will lead to larger energy separation between consecutive confined levels, which would decrease the probability of thermal carrier escape from the QDs to the QW and eliminate intermediary states for transfer of carriers from the lowest energy state in the QW to the QD GS.

SUPPLEMENTARY MATERIAL

See supplementary material for the layer sequence and band structure scheme; and details of numerical calculations.

ACKNOWLEDGMENTS

The work has been supported by the grant No. 2013/10/M/ST3/00636 of the National Science Centre in Poland and the QuCoS Project of Deutsche Forschungsgemeinschaft No. RE1110/16-1. The authors acknowledge technical support from Hamamatsu Co. with the near infrared streak camera apparatus.

[1] G. T. Liu, A. Stintz, H. Li, K. J. Malloy, and L. F. Lester, Electron. Lett. **35**, 1163 (1999).
[2] P. G. Eliseev, H. Li, T. Liu, T. C. Newell, L. F. Lester, and K. J. Malloy, IEEE J. Sel. Top. Quantum Electron. **7**, 135 (2001).
[3] M. V. Maksimov, N. Y. Gordeev, S. V. Zaitsev, P. S. Kop'ev, I. V. Kochnev, N. N. Ledentsov, A. V. Lunev, S. S. Ruvimov, A. V. Sakharov, A. F. Tsatsul'nikov, Y. M. Shernyakov, Z. I. Alferov, and D. Bimberg, Semiconductors **31**, 124 (1997).
[4] O. B. Shchekin and D. G. Deppe, Appl. Phys. Lett. **80**, 3277 (2002).
[5] S. Fathpour, Z. Mi, P. Bhattacharya, A. R. Kovsh, S. S. Mikhrin, I. L. Krestnikov, V. Kozhukhov, and N. N. Ledentsov, Appl. Phys. Lett. **85**, 5164 (2004).
[6] P. M. Varangis, H. Li, G. T. Liu, T. C. Newell, A. Stintz, B. Fuchs, K. J. Malloy, and L. F. Lester, Electron. Lett. **36**, 1544 (2000).
[7] Z. Mi, P. Bhattacharya, and S. Fathpour, Appl. Phys. Lett. **86**, 153109 (2005).
[8] Z. Mi and P. Bhattacharya, IEEE J. Quantum Electronics **42**, 1224 (2006).
[9] E. M. Pavelescu, C. Gilfert, J. P. Reithmaier, A. Martín-Mínguez, and I. Esquivias, IEEE Photon. Technol. Lett. **21**, 999 (2009).
[10] Z. Mi, P. Bhattacharya, and J. Yang, Appl. Phys. Lett. **89**, 153109 (2006).
[11] C. S. Lee, W. Guo, D. Basu, and P. Bhattacharya, Appl. Phys. Lett. **96**, 101107 (2010).
[12] J. Verma, S. M. Islam, V. Protasenko, P. K. Kandaswamy, H. Xing, and D. Jena, Appl. Phys. Lett. **104**, 021105 (2014).
[13] P. Bhattacharya, M. Zhang, and J. Hinckley, Appl. Phys. Lett. **97**, 251107 (2010).
[14] J. Kim, P. K. Kondratko, S. L. Chuang, G. Walter, N. Holonyak, Jr., R. D. Heller, X. B. Zhang, and R. D. Dupuis, Appl. Phys. Lett. **90**, 211102 (2007).
[15] C. Y. Jin, S. Ohta, M. Hopkinson, O. Kojima, T. Kita, and O. Wada, Appl. Phys. Lett. **96**, 151104 (2010).
[16] W. Rudno-Rudziński, G. Sęk, K. Ryczko, M. Syperek, J. Misiewicz, E. S. Semenova, A. Lemaitre, and A. Ramdane, Appl. Phys. Lett. **94**, 171906 (2009).
[17] S. Bhowmick, M. Z. Baten, T. Frost, B. S. Ooi, and P. Bhattacharya, IEEE J. Quantum Electron. **50**, 7 (2014).
[18] G. Sęk, P. Poloczek, P. Podemski, R. Kudrawiec, J. Misiewicz, A. Somers, S. Hein, S. Höfling, and A. Forchel, Appl. Phys. Lett. **90**, 081915 (2007).
[19] M. Syperek, J. Andrzejewski, W. Rudno-Rudziński, G. Sęk, J. Misiewicz, E. M. Pavelescu, C. Gilfert, and J. P. Reithmaier, Phys. Rev. B **85**, 125311 (2012).
[20] Yu. I. Mazur, V. G. Dorogan, E. Marega, Jr., Z. Ya. Zhuchenko, M. E. Ware, M. Benamara, G. G. Tarasov, P. Vasa, C. Lienau, and G. J. Salamo, J. Appl. Phys. **108**, 074316 (2010).
[21] Yu. I. Mazur, V. G. Dorogan, E. Marega, Jr., D. Guzun, M. E. Ware, Z. Y. Zhuchenko, G. G. Tarasov, C. Lienau, and G. J. Salamo, J. Appl. Phys. **113**, 034309 (2013).
[22] V. G. Talalaev, J. W. Tomm, N. D. Zakharov, P. Werner, U. Gösele, B. V. Novikov, A. S. Sokolov, Y. B. Samsonenko, V. A. Egorov, and G. E. Cirlin, Appl. Phys. Lett. **93**, 031105 (2008).
[23] V. G. Talalaev, G. E. Cirlin, B. V. Novikov, B. Fuhrmann, P. Werner, and J. W. Tomm, Appl. Phys. Lett. **106**, 013104 (2015).
[24] D. Gready and G. Eisenstein, IEEE J. Quantum Electron. **46**, 1611 (2010).
[25] D. S. Han and L. V. Asryan, Nanotechnology **21**, 015201 (2010).
[26] A. Mielnik-Pyszczorski, K. Gawarecki, and P. Machnikowski, Phys. Rev. B **91**, 195421 (2015).
[27] X. Yang, T. Kiba, T. Yamamura, J. Takayama, A. Subagyo, K. Sueoka, and A. Murayama, Appl. Phys. Lett. **104**, 012406 (2014).

[28] J. Pulka, T. Piwonski, G. Huyet, J. Houlihan, E. Semenova, A. Lematre, K. Merghem, A. Martinez, and A. Ramdane, Appl. Phys. Lett. **100**, 071107 (2012).
[29] A. Marent, T. Nowozin, M. Geller, and D. Bimberg, Semicond. Sci. Technol. **26**, 014026 (2011).
[30] G. Cerulo, L. Nevou, V. Liverini, F. Castellano, and J. Faist, J. Appl. Phys. **112**, 043702 (2012).
[31] G. L. Paravicini-Bagliani, V. Liverini, F. Valmorra, G. Scalari, F. Gramm, and J. Faist, New J. Phys. **16**, 083029 (2014).
[32] M. Z. M. Khan, T. K. Ng, C. S. Lee, P. Bhattacharya, and B. S. Ooi, Applied Phys. Lett. **102**, 091102 (2013).
[33] M. Z. M. Khan, M. Khan, T. K. Ng, and B. S. Ooi, Progress in Quantum Electronics **38**, 237 (2014).
[34] A. Sauerwald, T. Kümmell, G. Bacher, A. Somers, R. Schwertberger, J. P. Reithmaier, and A. Forchel, Appl. Phys. Lett. **86**, 253112 (2005).
[35] P. Podemski, R. Kudrawiec, J. Misiewicz, A. Somers, R. Schwertberger, J. P. Reithmaier, and A. Forchel, Appl. Phys. Lett. **89**, 151902 (2006).
[36] W. Rudno-Rudzinski, R. Kudrawiec, P. Podemski, G. Sęk, J. Misiewicz, A. Somers, R. Schwertberger, J. P. Reithmaier, and A. Forchel, Appl. Phys. Lett. **89**, 031908 (2006).
[37] M. Syperek, Ł. Dusanowski, M. Gawełczyk, G. Sęk, A. Somers, J. P. Reithmaier, S. Höfling, and J. Misiewicz, Appl. Phys. Lett. **109**, 193108 (2016).
[38] M. Syperek, Ł. Dusanowski, J. Andrzejewski, W. Rudno-Rudziński, G. Sęk, J. Misiewicz, and F. Lelarge, Appl. Phys. Lett. **103**, 083104 (2013).
[39] Ł. Dusanowski, M. Syperek, W. Rudno-Rudziński, P. Mrowiński, G. Sęk, J. Misiewicz, A. Somers, J. P. Reithmaier, S. Höfling, and A. Forchel, Appl. Phys. Lett. **103**, 253113 (2013).
[40] W. Rudno-Rudziński, G. Sęk, J. Andrzejewski, J. Misiewicz, F. Lelarge, and B. Rousseau, Semicond. Sci. Technol. **27**, 105015 (2012).
[41] C. Gilfert, E.-M. Pavelescu, and J. P. Reithmaier, Appl. Phys. Lett. **96**, 191903 (2010).